

COMITATO NAZIONALE PER L'ENERGIA NUCLEARE
Laboratori Nazionali di Frascati

LNF - 71/12
25 Marzo 1971

A. Cattoni, M. Piccolo and F. Ronga: A HIGH SENSITIVITY
METHOD FOR MEASURING MAGNETIC FIELD INTEGRALS.

A. Cattoni, M. Piccolo and F. Ronga: A HIGH SENSITIVITY METHOD FOR MEASURING MAGNETIC FIELD INTEGRALS. -

1. - INTRODUCTION -

One of the problems to be solved in the construction of a magnetic detector to be used at the storage ring Adone, is the interference of this detector with the magnets of the storage ring⁽¹⁾.

It is therefore necessary to have a means of measuring the field integral $\int B ds$ along the straight section occupied by the magnetic detector and nulling this field integral with compensator magnets.

An idea of the behaviour of the detector field, as seen by the stored beams, is given in fig. 1.

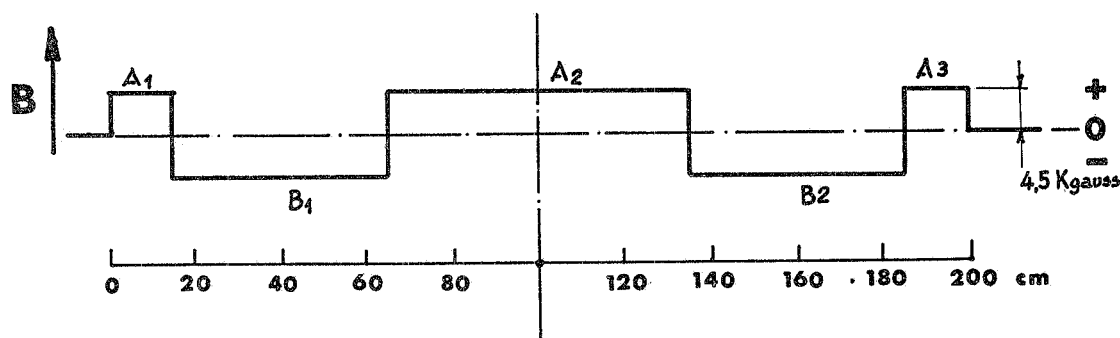


FIG. 1 - Field in the radial plane of Adone magnetic analyzer.

2.

The field in the segments A_1 , A_2 , A_3 is produced by the main coil, while the one at B_1 and B_2 is due to compensator magnets.

In order to avoid perturbations to the equilibrium orbit the following condition must to be satisfied:⁽²⁾

$$\int B ds \leq 2.5 \text{ gauss m} \quad (\text{at injection})$$

since the maximum available field for the main coil is 4.5 Kgauss the sensitivity of the magnetic field integral measurement must be at least 5×10^{-4} .

Any conventional field integral measurement using a (fixed) coil would not be faisible because of the size of the system and because it would not be possible in the available space to assure mechanical stability of the coil within the limits of the needed sensitivity.

For this reason we have decided to use an electromagnetic balance consisting of a current carrying wire sensed by two piezoelectric crystals.

2. - EXPERIMENTAL SET UP -

The method has been tested by a prototype consisting essentially of a copper wire, 5 mm in diameter stretched along the internal axis and fixed at either end of a tube, with a rectangular cross section, 2.5 m in lenght. Tube and wire are supported at the ends by two quartz crystals (see fig. 2), which measure the force component in the x-axis direction.

Four bronze-phosphorous strips, fixing the tube to a U support, prevent it from moving in the y-axis direction.

A block scheme of the instrument is shown in fig. 3.

A low frequency oscillator (0.5 - 1.5 Hz) drives a power amplifier at the output of which there is a trasformer with turns ratio 25 : 1 and band pass 0.3 - 10 hz; the resulting low frequency current flowing in the wire is about 70 amps. If the wire lies in a magnetic field directed along y direction, there is a force acting on the wire which varies sinusoidally in the x direction and, in the very low frequency limit, is proportional to the integral of B_y along the wire.

The characteristics of piezoelectric crystals are listed in Table I.

In our series of tests the force on the wire when a 1 Gauss magnetic field is applied was 1.7 gr. considerably more than crystal's resolution, which is 0.1 gr.

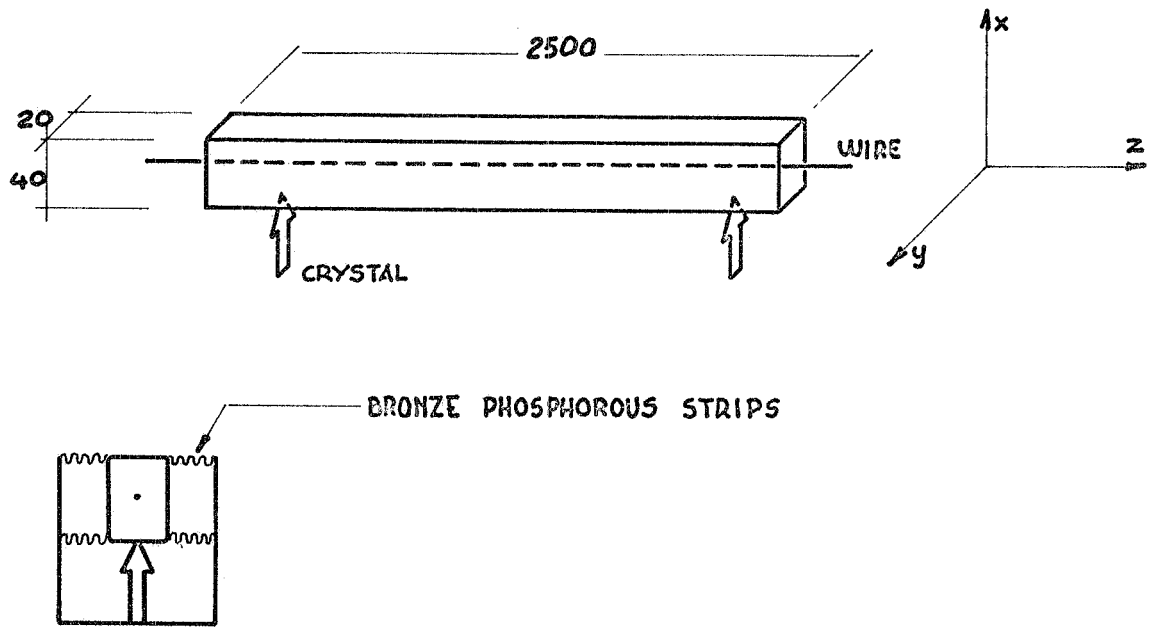


FIG. 2 - Magnetometer scheme

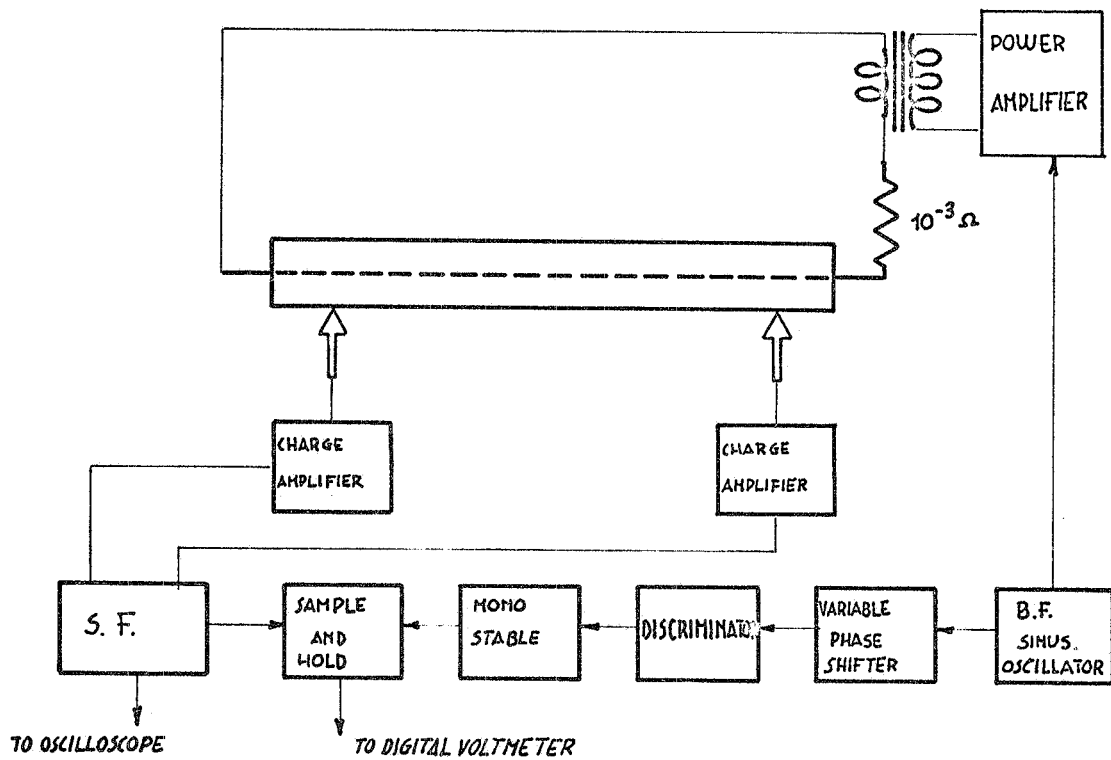


FIG. 3 - Block diagram

TABLE I

Quartz Force Transducers Kistler 9201	
Max measuring range	+ 50 kp - 0.1 gp
Resolution	480 pC/Kp
Sensitivity	12 μ m
Deformation at max load	+ 0.3%
Linearity	- $10^{14} \Omega$
Insulation resistance	22 pf
Capacity	

Crystal's outputs are connected to charge amplifiers (using MOSFET, Philips type TAA 320) having input impedances $10^{11} \Omega$. The SF circuit indicated in fig. 3 sums output signals and provides suitable filtering through two double T serial filters. The band width of a typical filter we have used is shown in fig. 4.

It is necessary to use filters owing to the background of the crystals output signals resulting from floor vibration and acoustical pickup. Furthermore, as we will later discuss, the filters are needed to reject those signals, two three four times the excitation frequency which are produced by magnetic field gradients. In designing filters care must be taken to obtain a narrow band pass as well as a fast rise time. The filter shown in fig. 4 has a rise time of 2-3 sec. The sum circuit output is fed into a classical sample-and-hold circuit in order to have a d.c. level at the output of the instrument. This sample-and-hold circuit is driven by an other one which consists of a phase shifter, a discriminator and a monostable, in order to sample the input peak signal.

3. - MAGNETOMETER'S RESPONSE -

The response of any dynamical system, subject to time dependent forces, in the absence of dumping, has poles at the resonating frequencies.

The time dependent forces applied to a system are transmitted without any dynamical contribution, only if the driving frequency is much less than the first resonance of the dynamical system.

Our instrument described in the previous paragraphs consists of three oscillating systems:

- a) clamped field sensing wire
- b) sustaining tube

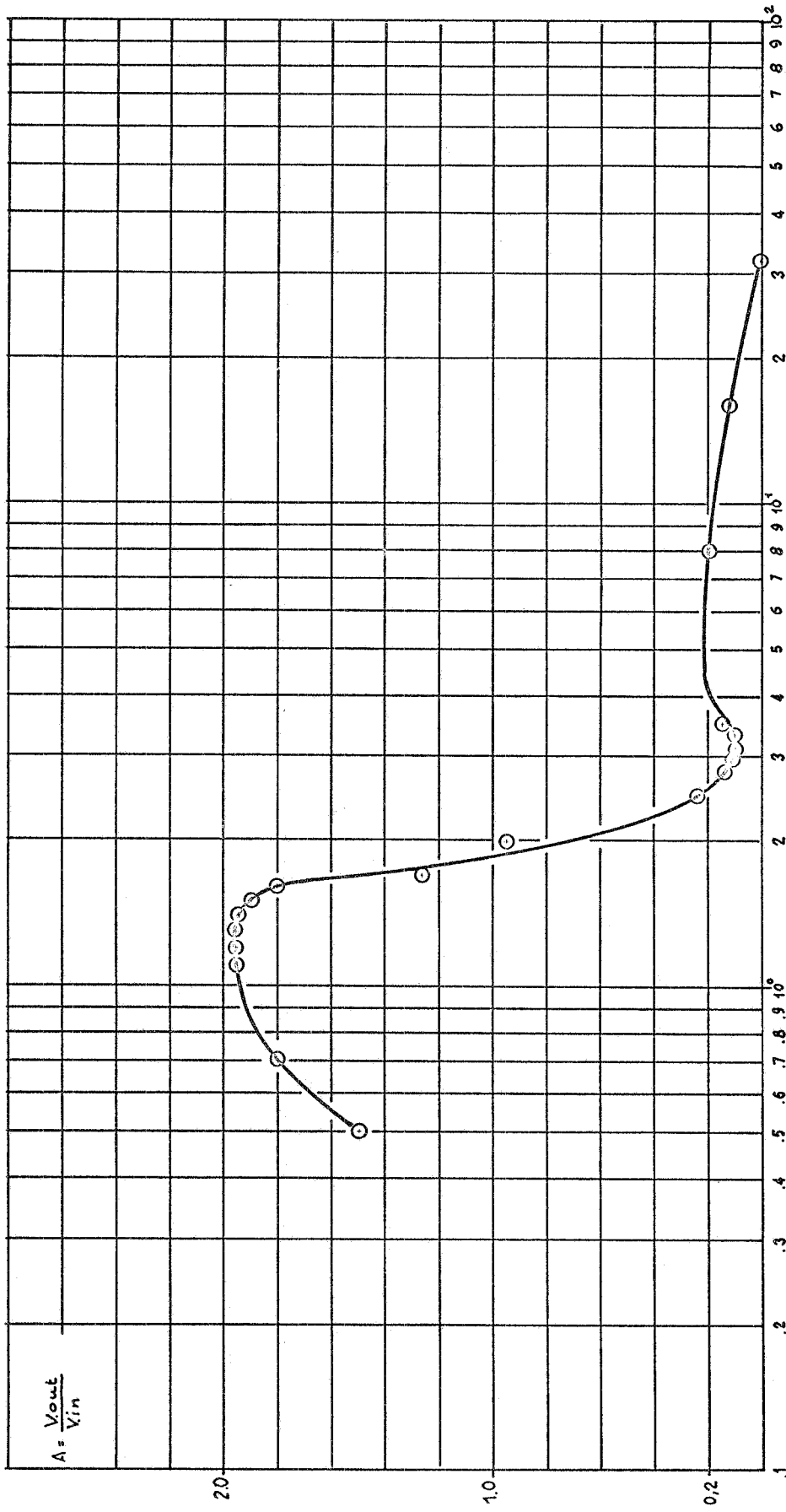


FIG. 4 - Frequency response of a typical filter.

6.

c) U-support

In table II resonant frequencies are listed corresponding to two distinct values of the wire mechanical tension.

TABLE II
Resonant frequencies of the magnetometer.

82 Kg.	140 Kg.	ν_{140} / ν_{82}
15,5	20	1,29
31,5	39	1,27
48	60	1,25
61	63	1,06
67	84	1,25
115	115	1,00

There are two frequencies that are independent of the wire's tension and therefore are due to the mechanical structure of the support.

The table shows also that the dynamical response of the system, within the range 0 - 60 Hz is completely determined by the wire; hence we can schematically represent the magnetometer just as a vibrating string. The equation which describes a string of length L, subject to a force $f(x, t)$ per unity length, normal to its axis, is

$$(1) \quad T \frac{\partial^2 \eta}{\partial x^2} + f(x, t) = \mu \frac{\partial^2 \eta}{\partial t^2}$$

where T is the mechanical tension, η is the wire displacement and μ is the wire linear density.

If we put

$$f(x, t) = F(x) e^{i \omega t}$$

and

$$\eta(x, t) = a(x) e^{i \omega t}$$

we obtain from (1)

$$(2) \quad \frac{d^2 a}{dx^2} = -g^2 a - \frac{F(x)}{T}$$

where

$$g = \frac{\pi \nu}{L \nu_0} \quad \nu_0 = \frac{1}{2L} \sqrt{\frac{T}{\mu}} \quad \nu = \frac{\omega}{2\pi}$$

For a given force distribution $F(x)$ the resultant constraint forces, R is

$$(3) \quad R = T \left[\left. \frac{da}{dx} \right|_{x=L} - \left. \frac{da}{dx} \right|_{x=0} \right]$$

In the case of step distribution of forces:

$$\begin{aligned} F(x) &= 0 & 0 < x < x_1 \\ F(x) &= F & x_1 < x < x_2 \\ F(x) &= 0 & x_2 < x < L \end{aligned}$$

we obtain

$$(4) \quad R = \frac{F}{g} \left[(-\text{seng}x_2 - \text{seng}x_1) - (\text{cos}gx_1 - \text{cos}gx_2) \frac{1 - \text{cos}gL}{\text{seng}L} \right]$$

$$(5) \quad R_{gL} \underset{\rightarrow 0}{\sim} F \left[-(x_2 - x_1) + (gL)^2 L \left(\frac{x_2^3 - x_1^3}{6L^3} - \frac{x_2^2 - x_1^2}{4L^2} \right) \right]$$

Equation (5) shows that the resultant constraint forces is equal to the integral of $F(x)$ (which corresponds to a static term) plus a dynamical term proportional to the square of the excitation frequency.

The linearity of equation (1) allows to apply the superposition principle for any arbitrary force distribution. For instance in the case of fig. 5 if we apply equation (5) to each step and sum the results we get (since the integral of B is zero)

$$(6) \quad R = -iB(gL)^2 \frac{L}{32}$$

where B is the magnetic field applied and i is the current flowing in the wire. If we want

$$\frac{R}{iB \frac{L}{2}} \leq 5 \times 10^{-4}$$

we obtain if $L = 2,5$ m.

8.

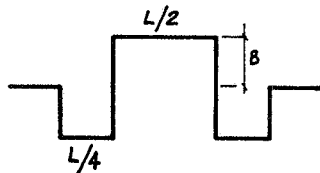
$$(7) \quad v \leq \frac{v_0}{35}$$

If there is dumping with viscosity constant per unity length ξ , we have to substitute in equation (5) for g^2

$$(8) \quad g'^2 = g^2 - j \frac{\omega \xi}{T}$$

In our case the dumping constant of the wire when no magnetic field is present, is

$$(9) \quad \xi = 10^{-2} \text{ new x sec/m}^2$$



that is at very low frequencies, the correction is small and the time constant of the dumping is about 25 sec.

When there is a magnetic field, there is a force per unity length due to induced currents given by

$$(10) \quad F'(x) = -j \frac{\omega B(x)}{Z} \int_0^L a(x) B(x) dx$$

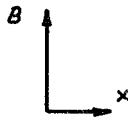


FIG. 5

where $Z = R + j\omega L$ is the impedance of the circuit closed by the wire and $a(x)$ is the wire displacement.

Since in our case ($\omega = 3.14 \text{ sec}^{-1}$) Z is a pure resistance, $F'(x)$ is 90° out of phase with the excitation and therefore does not affect the measurement.

The dumping effect of $F'(x)$ is quite strong: experimentally we have proved that in our conditions (see next paragraph for details of the applied field) when the integral is zero the time constant for free oscillation dumping is 2 sec.

Owing to dynamical displacement the wire grows longer with a subsequent tension change: equation (1) can be modified to take into account tension terms resulting from dynamical displacement in the wire:

$$(11) \quad (T + \frac{ES}{2L} \int_0^L (\frac{\partial \eta}{\partial x})^2 dx) \frac{\partial^2 \eta}{\partial x^2} + f(x, t) = \mu \frac{\partial^2 \eta}{\partial t^2}$$

We can solve (11) with perturbative methods setting

$$(12) \quad \eta(x, t) = \eta_0(x, t) + \beta(x, t)$$

where $\eta_0(x, t)$ is the solution of (1), $\beta(x, t)$ is the correction. It can be shown that the resultant of the constrain forces is independent of $\beta(x, t)$.

If magnetic gradients are present in the region spanned by the wire one must also take into account the presence of corrective terms:

$$(13) \quad f(x, t) = B(x, 0)i(t) + \left. \frac{\partial B}{\partial a} \right|_{a=0} i(t)a(x)\text{sen}\omega t + \frac{1}{2} \left. \frac{\partial^2 B}{\partial a^2} \right|_{a=0} i(t)a^2(x)\text{sen}^2\omega t + \dots$$

from which

$$(14) \quad f'(x, t) = \left. \frac{\partial B}{\partial a} \right|_{a=0} i_0 a^2(x) + \left[B(x, 0) + \left. \left(\frac{\partial^2 B}{\partial a^2} \right) \right|_{a=0} \frac{3a^2(x)}{8} \right] x$$

$$x i_0 \text{sen}\omega t - \left. \frac{\partial B}{\partial a} \right|_{a=0} i_0 \frac{a(x)\cos 2\omega t}{2} + \dots$$

In our case the results are: (see next paragraph)

$$\text{I} \quad \int_0^L \left. \frac{\partial^2 B}{\partial a^2} \right|_{a=0} a^2(x) dx = 0.08 \text{ gauss x meter}$$

$$\text{II} \quad \int_0^L \left. \frac{\partial B}{\partial a} \right|_{a=0} a(x) dx = 10 \text{ gauss x meter}$$

It is therefore necessary (as we see from the size of the term II) to achieve an high rejection of the second harmonic excitation frequency; typically with the filters we have used the rejection is about 15 : I and satisfactory.

4. - EXPERIMENTAL TESTS -

In order to obtain the absolute calibration of the magnetometer, we have made measurement in the magnetic field produced by a thin copper bar three meters long parallel to the wire (fig. 6).

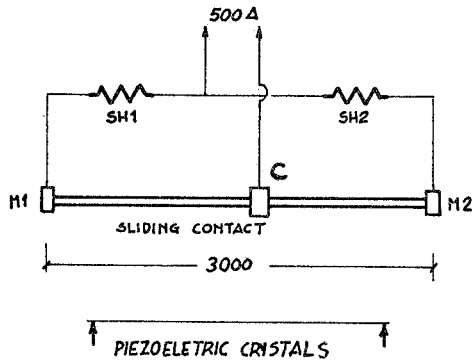


FIG. 6 - Scheme of calibration disposal.

The linearity of the system as a function of the current flowing in the bar between M_1 and M_2 is shown in fig. 7.

In fig. 8 we show the behaviour of the signal from the magnetometer as a function of the field integral, which we have calculated from the values of the shunts SH_1 and SH_2 .

Obviously there is a position of the contact C corresponding to

$$\int \underline{B} \times d\underline{l} = 0$$

In this condition also the output signal, after subtraction of coherent background, is zero.

From the graph. of fig. 7 it is possible to determine the value of this background (~ 0.5 gauss x meter) which is due essentially to the earth's magnetic field and small stray fields from nearby conductors.

We have also carried out measurement using a row of three magnets arranged in such a way to simulate working conditions of the magnetometer. The fig. 9 shows the scheme of powering the magnets while fig. 10 displays the field configuration used.

As can be seen from eq. (5-3), if the integral of the field is zero the magnetometer output will be zero only in the low frequency limit. This effect and the expected frequency dependence was experimentally tested and is described below.

The field integral is brought to zero by means of the variable shunt SV (see fig. 9) which takes up about 10% of the current of M_c . M_1 and M_2 are magnets with level and parallel poles, while M_c is a magnet having $\partial B / \partial y = 50$ Gauss/cm.

Measurements were carried out as follows: SV was set in order to obtain zero output at drive frequency of 0.5 Hz. Then for each different value of the excitation frequency, we have measured output voltage normalizing by filter response.

The ratio of this voltage to the one obtained when only M_c is on, is plotted against the square of the frequency (fig. 11). The slope of the

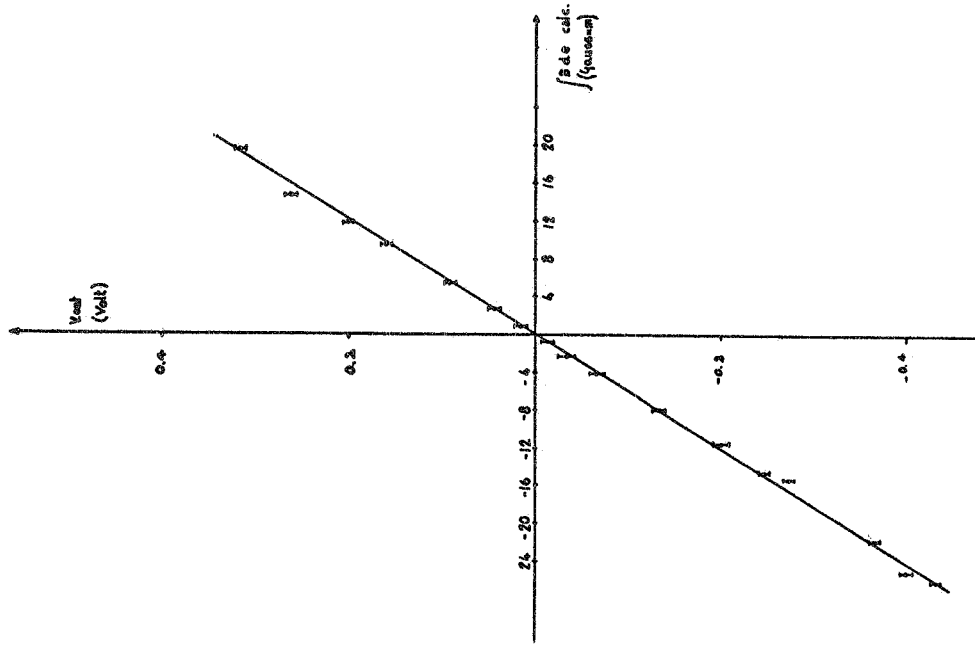


FIG. 8 - Magnetometer's output versus sliding contact position.

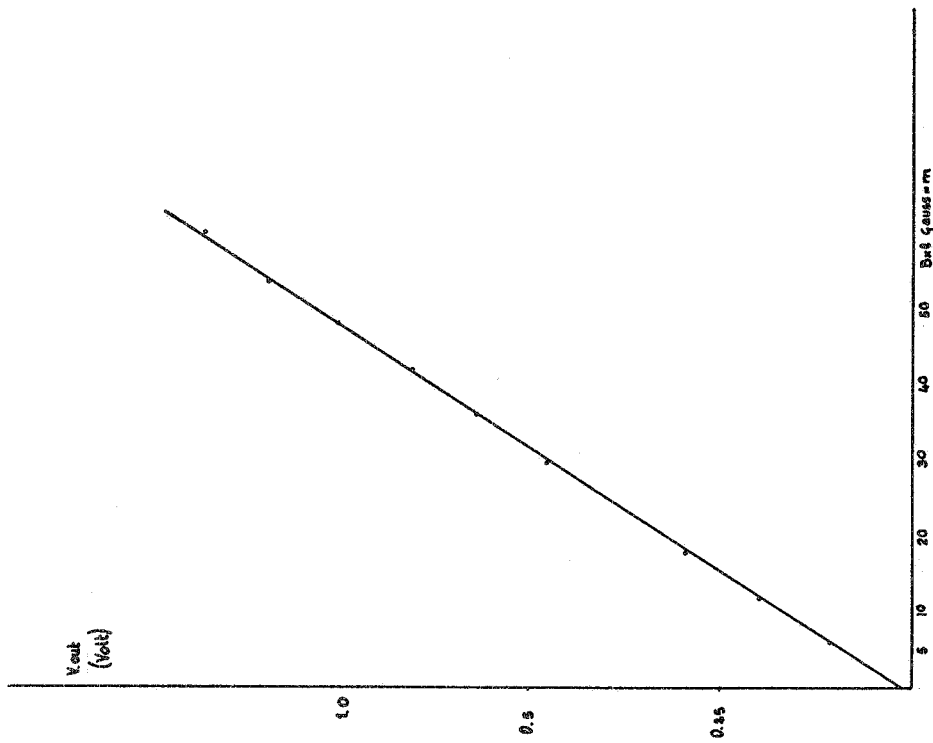


FIG. 7 - Magnetometer's output versus bar current

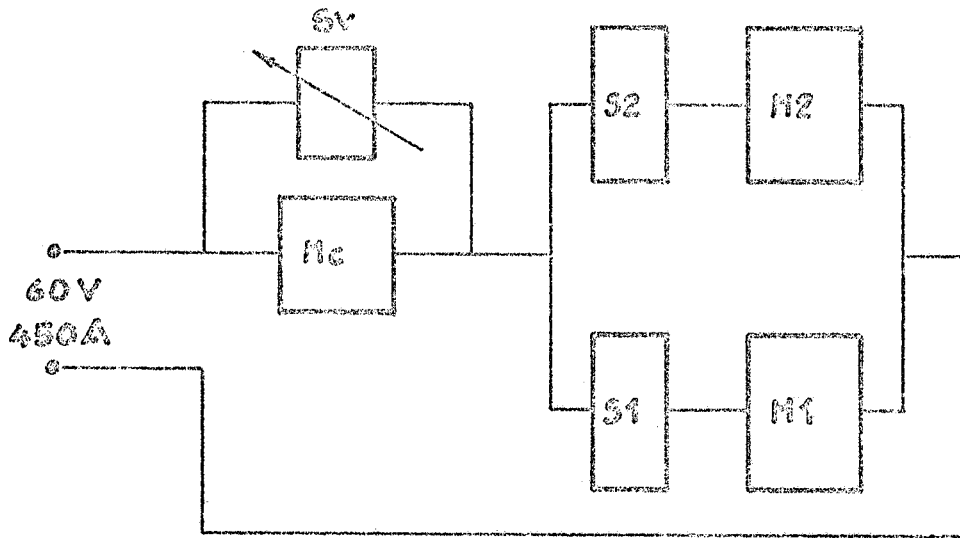


FIG. 9 - Scheme of powering the magnets.

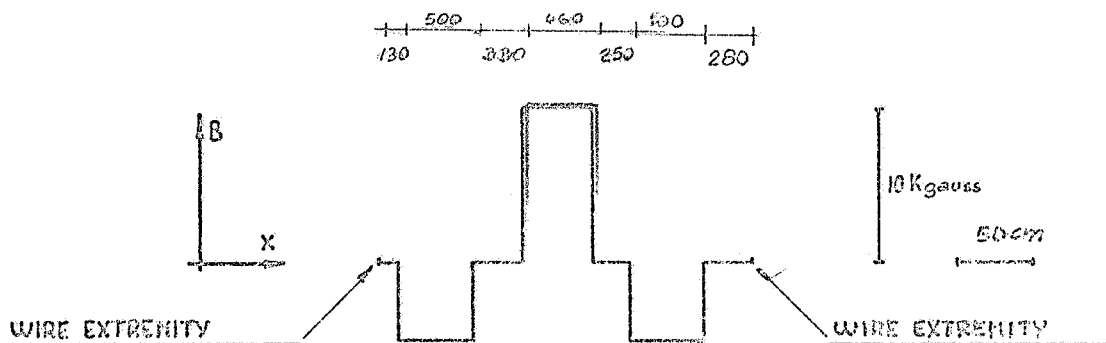


FIG. 10 - Field configuration in the row of the magnets.

straight line which fits experimental points is $1.86 \times 10^{-3} \text{ Hz}^{-2}$; this value is to be compared with the calculated value $1.77 \times 10^{-3} \text{ Hz}^{-2}$ that we obtain if equation (3-5) is applied to each field segment.

Taking into account the approximation we made (step behaviour of magnetic fields, induced currents in the wire, etc.), we can be satisfied with this agreement between theoretical and experimental points. Furthermore we have to consider the effects from the power supply and shunt instabilities; we have tried to minimize these effects with repetition and averaging measurements.

The results we have obtained allow us be confident, that our scheme as described in the previous paragraph, is completely correct.

In particular, we have found that the behaviour of the magnetometer does not depend on the resonating frequency of the wire within 5×10^{-4} (when the magnets are arranged as in fig. 10), if the following

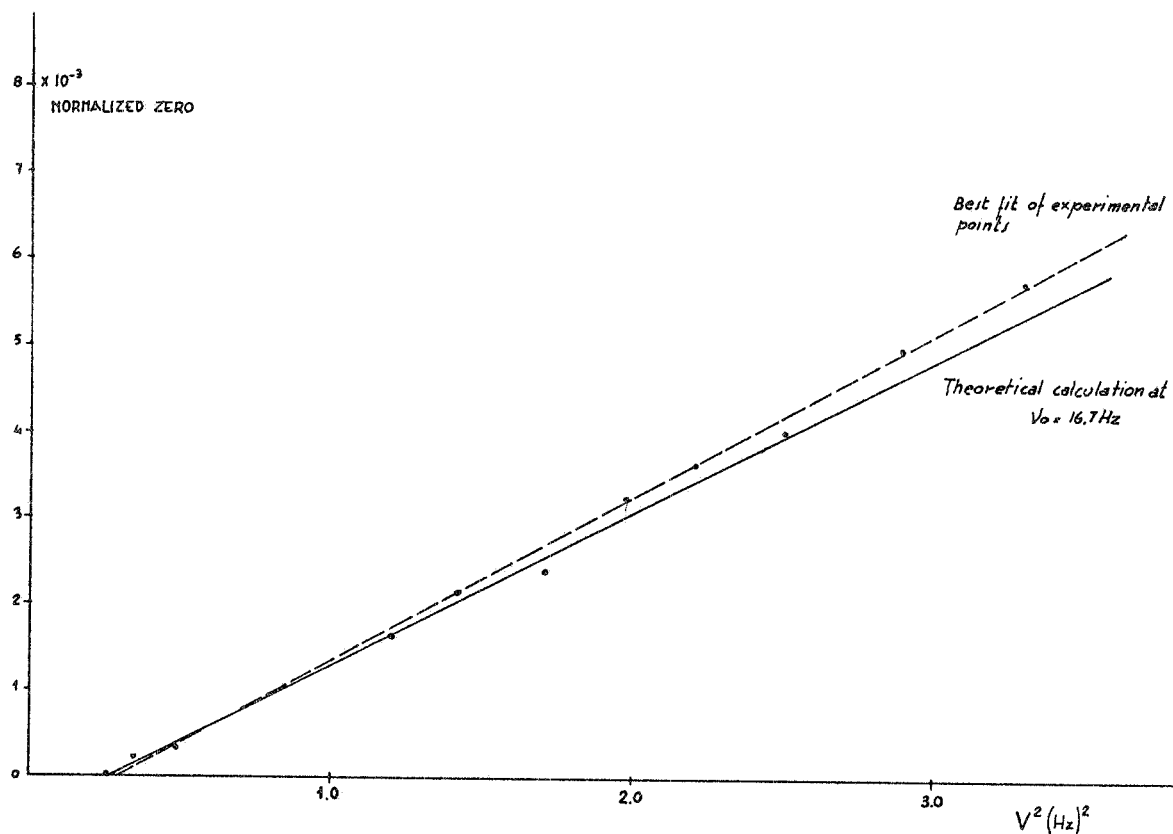


FIG. 11 - Normalized zero versus frequency square.

condition is fulfilled:

$$v \leq \frac{v_0}{45} .$$

5. - CONCLUSIONS -

The measuring method we have suggested is as sensitive as is required, however our tests on the prototype allow us to plan the following improvements to be carried out when the final magnetometer will be built:

a) wire will be made of aldry so the first resonating frequency will be about 50 Hz.

b) one of the extremities of the wire will be connected to a spring (see fig. 12) in order to increase the stability of the mechanical tension.

c) the support will be made more rigid to reduce distorsions and allow an higher tension in the wire.

Furthermore we hope to achieve a great improvement in the si-

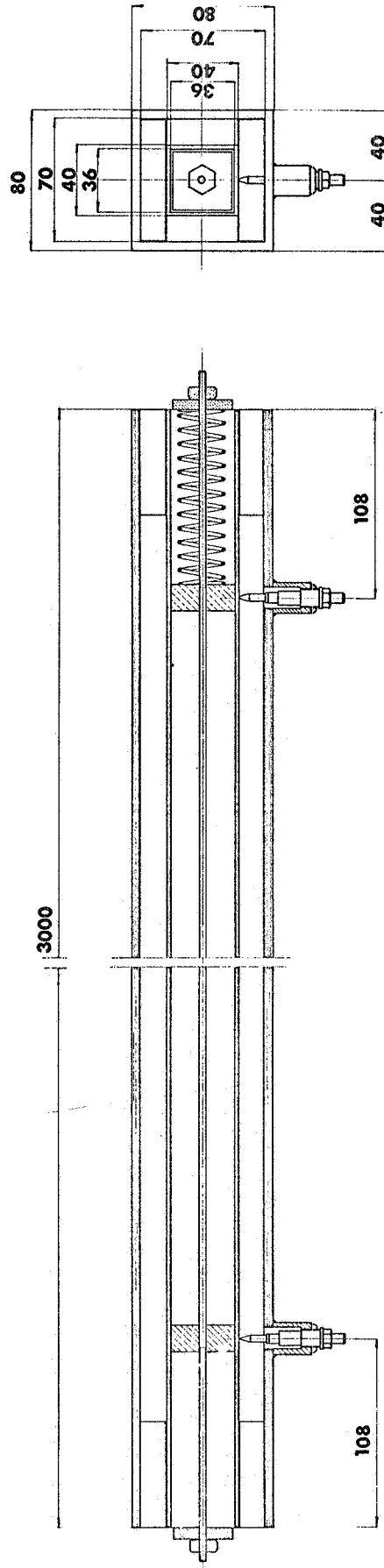


FIG. 12 - Final magnetometer project

gnal to noise ratio by using a voltage correlator.

ACKNOWLEDGEMENTS -

It is a pleasure for us to thank Dr. W.W. Ash for his collaboration.

We are also indebted to prof. V. Silvestrini and Dr. B. Bartoli for their usefull suggestions.

REFERENCES -

- (1) - W.W. Ash et al., A magnetic analyzer to be used for Adone colliding beam experiments. LNF-69/2 (1969).
- (2) - F. Amman, Private communication.